SLAC-PUB-10152
August 2003
hep-ph/0307158

Inclusive $|V_{ub}|$ Measurements at *BABAR*

A. Sarti

Representing the *BABAR* Collaboration

Invited talk presented at the 2nd Workshop on the CKM Unitarity Triangle,
4/5/2003—4/9/2003, Durham, England

Stanford Linear Accelerator Center, Stanford University, Stanford, CA 94309

Work supported by Department of Energy contract DE–AC03–76SF00515.

Workshop on the CKM Unitarity Triangle, IPPP Durham, April 2003

Inclusive $|V_{ub}|$ measurements at *BABAR*

A Sarti on behalf of the *BABAR* Collaboration

Università di Ferrara, Dipartimento di Fisica and INFN, I-44100 Ferrara, Italy

We present two inclusive measurements of Cabibbo-Kobayashi-Maskawa (CKM) matrix element $|V_{ub}|$: one uses the lepton energy spectrum (E_l) and the other uses the invariant mass of the hadronic system (m_X) to discriminate signal ($\overline{B} \to X_u \ell \overline{\nu}$) and background ($\overline{B} \to X_c \ell \overline{\nu}$) events in $\overline{B} \to X \ell \overline{\nu}$ transitions. Both analyses are based on data samples collected by the *BABAR* detector at the PEP-II asymmetric-energy B Factory at SLAC.

The element $|V_{ub}|$ of the CKM matrix [1] plays a central role in tests of the unitarity of this matrix: it's extraction, based on tree level decays, gives results that are independent of new physics contributions. We report the determination of $|V_{ub}|$ from two different measurements of the inclusive charmless semileptonic B branching fraction, $\mathcal{B}(\overline{B} \to X_u \ell \overline{\nu})$[1], using E_l spectrum (endpoint) and the m_X spectrum on the recoil of fully reconstructed B mesons respectively.

The selection of $\overline{B} \to X_u \ell \overline{\nu}$ events is hampered by the presence of a large $\overline{B} \to X_c \ell \overline{\nu}$ background: E_l and m_X spectra are used to discriminate the two different transitions. The endpoint analysis is sensitive to approximately 10% of the E_l spectrum while the acceptance for the m_X approach is larger: $\simeq$ 70% of the m_X spectrum is selected by analysis cuts. The extrapolation of the measured rates to the full phase space introduces theoretical uncertainties[2][2]. Results also depend on the shape function (SF) modeling of b quark Fermi motion inside the B meson.

Both measurements are based on data recorded by the *BABAR* detector [3] at the PEP-II asymmetric-energy e^+e^- storage ring at SLAC. The endpoint analysis data sample consists of about 23 million $B\overline{B}$ pairs (21 fb^{-1}) collected at the $\Upsilon(4S)$ resonance (ON-peak), with an additional sample of 2.6 fb^{-1} recorded about 40 MeV below the $\Upsilon(4S)$ peak (OFF-peak), while the m_X measurement uses a data sample of about 88 million $B\overline{B}$ pairs (82 fb^{-1}) ON-peak.

Monte Carlo (MC) simulations of the *BABAR* detector based on `GEANT 4` [4] are used to optimize selection criteria and to determine signal efficiencies and background shapes. To simulate $\overline{B} \to X_c \ell \overline{\nu}$ transitions three models are employed: $\overline{B} \to D^* \ell \nu$ decay is modeled following a parametrization of form factors based on HQET [5]; for $\overline{B} \to D \ell \nu$ decays and higher mass charm meson states $\overline{B} \to D^{(**)} \ell \overline{\nu}$ the ISGW2 model [6] is used; nonresonant decays, $\overline{B} \to D^{(*)} \pi \ell \nu$, are modeled according to a prescription by Goity and Roberts [7]. In the endpoint analysis the MC simulation of $\overline{B} \to X_u \ell \overline{\nu}$ events is based on the ISGW2 model: the hadrons X_u are represented by single particles or resonances with masses up to 1.5 GeV/c^2 and nonresonant contributions are not included. In the m_X analysis $\overline{B} \to X_u \ell \overline{\nu}$ transitions are simulated with an hybrid model which is a mixture of resonant and nonresonant components. The Fermi motion of the b quark inside the B meson is implemented in the nonresonant component using the SF parameterization described in [8], and the fragmentation is handled by `Jetset7.4` [9].

1 Endpoint analysis

For this analysis, electron candidates are selected in the momentum range from 1.5 to 3.5 GeV/c in the $\Upsilon(4S)$ rest frame with a solid angle defined by the electromagnetic calorimeter acceptance.

The inclusive electron spectrum for charmless semileptonic B decays, measured in the $\Upsilon(4S)$ rest frame in the momentum range of 2.3–2.6 GeV/c, is used to extract $\mathcal{B}(\overline{B} \to X_u \ell \overline{\nu})$. To suppress low-multiplicity QED processes and continuum processes consisting of nonresonant $e^+e^- \to q\overline{q}$ production ($q = u, d, s, c$) at least three charged tracks per event are required and a cut on the ratio of Fox-Wolfram moments $H_2/H_0 < 0.4$ [10] is applied. The missing momentum four-vector $p_{miss} = p_i - p_{B_{reco}} - p_X - p_\ell$, where all momenta are measured in the laboratory frame and p_i refers to the four-momentum of the initial state of the colliding beams, can be used to select semileptonic events: $|p_{miss}|$ is requested to be larger than 1 GeV/c, to point into the detector fiducial volume and the angle between the electron candidate and the missing momentum is required to be greater than $\pi/2$. Candidate electrons are rejected if, when paired with an opposite-sign electron, the invariant mass of the pair is consistent with the J/ψ mass ($3.05 < M_{e^+e^-} < 3.15$ GeV/c^2). For the selection criteria described above, the detection efficiency for charmless semileptonic decays in the electron momentum interval of 1.5 – 2.6 GeV/c ranges from ~ 0.4 to ~ 0.25.

The raw spectrum of the highest momentum electron after the subtraction of continuum background (determined from OFF resonance data sample) is shown in Fig. 1a. Also

[1] Charge-conjugate states are implied throughout this paper.

[2] The results presented are depending on the parton-duality to which no error is assigned.

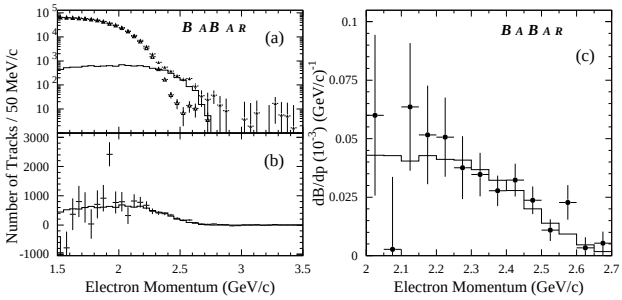

Figure 1. Electron momentum spectrum in the $\Upsilon(4S)$ rest frame. (a) ON-peak data after continuum subtraction (solid triangles), and MC predicted background from $B\bar{B}$ events ($B \nrightarrow X_u e\nu$) (open triangles). (b) ON peak data after subtraction of continuum and MC predicted $B \nrightarrow X_u e\nu$ backgrounds (data points with statistical errors). For comparison, the histograms show the expected signal spectrum from $B \to X_u e\nu$ decays. (c) The differential rate $\mathcal{B}(B \to X_u e\nu)$ as a function of the electron momentum. The data (statistical errors only) are compared to the prediction (solid line).

shown are the MC predictions of the expected signal from $\overline{B} \to X_u e\overline{\nu}$ decays and background contributions from all other processes. The result of the subtraction of all backgrounds is shown in Fig. 1b. For a given interval in the electron momentum, the inclusive partial branching ratio is calculated according to

$$\Delta\mathcal{B} = \frac{N_{\rm ON} - N_{\rm OFF} - N_{B\nrightarrow X_u e\nu}}{2\epsilon N_{B\bar{B}}}(1+\delta_{rad}). \qquad (1)$$

Here $N_{\rm ON}$ refers to the number of electrons detected ON-peak and $N_{\rm OFF}$ refers to the fitted continuum background in a specified momentum interval, $N_{B\nrightarrow X_u e\nu}$ is the background from $B\bar{B}$ decays, ϵ is the total efficiency for detecting a signal electron from $B \to X_u e\nu$ decays (including bremsstrahlung in detector material), and δ_{rad} accounts for the distortion of the electron spectrum due to final-state radiation. As the overall normalization the total number of produced $B\bar{B}$ events is used, $N_{B\bar{B}} = (22,630 \pm 19 \pm 362)\cdot 10^3$. The systematic error introduced by the efficiency estimation for the signal events is 5%. The uncertainty in the continuum background subtraction is 5%. The error coming from the $B\bar{B}$ background modeling translates to a relative error of 3%. Variations of the colliding beam energy introduce a systematic error in the $B \to X_c e\nu$ background subtraction (5%). The total systematic error on the partial branching ratio measurement is $\sim$ 9%.

The fully corrected differential branching ratio as a function of the electron momentum is shown in Fig. 1c. Integrating over the interval from 2.3 to 2.6 GeV/c, we get:

$$\Delta\mathcal{B}(B \to X_u e\nu) = (0.152 \pm 0.014 \pm 0.014)\cdot 10^{-3} \qquad (2)$$

To determine the charmless semileptonic branching fraction $\mathcal{B}(B \to X_u e\nu)$ from the partial branching fraction $\Delta\mathcal{B}(\Delta p)$, the fraction $f_u(\Delta p)$ of the spectrum that falls into the momentum interval Δp is needed. The CLEO collaboration has recently used the measurement of the inclusive photon spectrum from $b \to s\gamma$ transitions [11] to derive $f_u(\Delta p)$ for $B \to X_u e\nu$ transition. They quote a value of $f_u(\Delta p) = 0.074 \pm 0.014 \pm 0.009$ for the interval Δp from 2.3 to 2.6 GeV/c. Relying on the CLEO measurement, the result presented here translates into a total branching ratio of $\mathcal{B}(B \to X_u e\nu) = (2.05 \pm 0.27_{exp} \pm 0.46_{f_u})\cdot 10^{-3}$. We extract $|V_{ub}|$ from the measured inclusive charmless semileptonic branching fraction with the relation in [15] and the average B lifetime of $\tau_B = 1.608 \pm 0.012$ ps [15] and find

$$|V_{ub}| = (4.43 \pm 0.29_{exp} \pm 0.25_{OPE} \pm 0.50_{f_u} \pm 0.35_{s\gamma})\cdot 10^{-3} \qquad (3)$$

Here the first error is the combined statistical and systematic error, and the second refers to the uncertainty on the extraction of $|V_{ub}|$ from relation in [15]. The third one is taken from the CLEO analysis and is related to the experimental determination of f_u. The last error accounts for uncertainties related to assumption that $b \to s\gamma$ spectrum can be used for shape function modeling in $B \to X_u e\nu$ transition.

2 $|V_{ub}|$ measurement using the recoil of fully reconstructed B mesons

This analysis is based on $B\overline{B}$ events in which one of the B meson decays in a fully reconstructed hadronic final state (B_{reco}) and the other one is identified as decaying semileptonically by the presence of an electron or a muon. The full reconstruction of one of the two B mesons reduces the overall efficiency, but allows to reconstruct both the neutrino and the hadronic system (X), to determine the flavour and to separate charged and neutral B mesons. In order to reduce systematic uncertainties due to efficiency determination we extract the branching ratio $R_{u/sl} = \mathcal{B}(\overline{B} \to X_u \ell\overline{\nu})/\mathcal{B}(\overline{B} \to X\ell\overline{\nu})$ after measuring the number of events with one identified lepton.

To fully reconstruct a large sample of B mesons, hadronic B decays of the type $B_{reco} \to D^{(*)}Y$ are selected. Y represents a collection of hadrons with a total charge of ± 1, composed of $n_1\pi^\pm\, n_2 K^\pm\, n_3 K_s^0\, n_4\pi^0$, where $n_1 + n_2 < 6$, $n_3 < 3$, and $n_4 < 3$. The kinematic consistency of a B_{reco} candidate with a B meson decay is checked using two variables, the beam energy-substituted mass $m_{\rm ES} = \sqrt{s/4 - \vec{p}_B^{\,2}}$ and the energy difference, $\Delta E = E_B - \sqrt{s}/2$. Here $\sqrt{s}$ refers to the total energy in the $\Upsilon(4S)$ center of mass frame, and $\vec{p}_B$ and E_B denote the momentum and energy of the B_{reco} candidate in the same frame, respectively. In events with more than one reconstructed B decay, the decay mode with highest purity is selected.

Semileptonic $\overline{B}$ decays, $\overline{B} \to X\ell\overline{\nu}$, recoiling against the B_{reco} candidate are identified by an electron or muon candidate with a minimum momentum (p^*) greater than 1 GeV/c

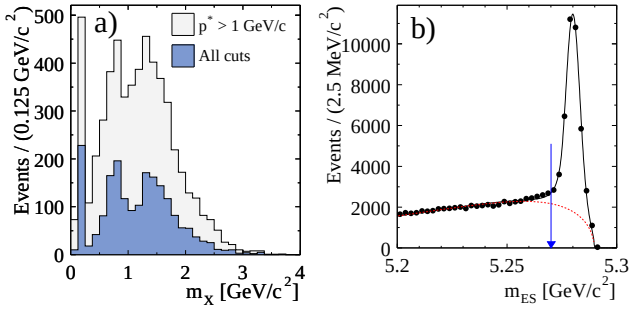

Figure 2. a) Signal MC m_X distributions with the requirement of a lepton with $p^* > 1\,\mathrm{GeV}/c$. Measured m_X distribution before and after all cuts. b)Fit to the m_{ES} distribution for the lepton sample with $p^* > 1\,\mathrm{GeV}/c$ in the recoil of a B_{reco} candidate

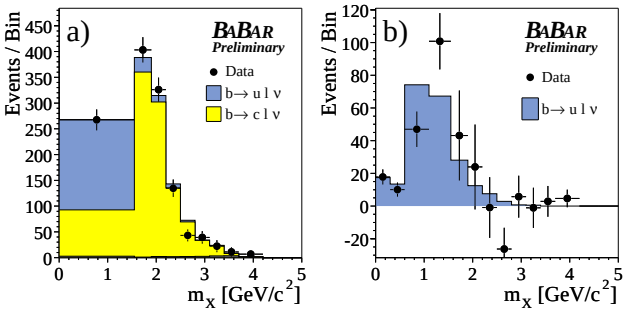

Figure 3. The m_X distribution in $\overline{B} \to X\ell\overline{\nu}$ decays. a) Data (dots) and fit components. b) Background subtracted data and signal MC.

in the $\overline{B}$ rest frame. Correlation between the charge of the prompt leptons and the flavor of the B_{reco} is imposed ($B^0 - \overline{B}^0$ mixing rate is used to extract the prompt lepton yield in case of neutral candidates).

The hadron system X in the decay $\overline{B} \to X\ell\overline{\nu}$ is made of charged tracks and neutral energy depositions in the calorimeter that are not associated with the B_{reco} candidate and not identified as a lepton. The mass of the hadronic system is determined by a kinematic fit that imposes four-momentum conservation, the equality of the masses of the two B mesons, and forces $p^2_{miss} = 0$.

The selection of $\overline{B} \to X_u\ell\overline{\nu}$ decays is tightened by requiring exactly one charged lepton with $p^* > 1\,\mathrm{GeV}/c$, charge conservation ($Q_X + Q_\ell + Q_{B_{reco}} = 0$), and missing mass consistent with zero ($p^2_{miss} < 0.5\,\mathrm{GeV}^2/c^4$). These criteria improve the resolution in m_X and suppress the dominant $\overline{B} \to X_c\ell\overline{\nu}$ decays, many of which contain additional neutrinos or undetected K_L. We suppress the $\overline{B}^0 \to D^{*+}\ell^-\overline{\nu}$ background with a partial reconstruction in which only the slow pion from the $D^{*+} \to D\pi^+_s$ decay and the lepton are reconstructed. We veto events with charged or neutral kaons in the X system to reduce the background from $\overline{B} \to X_c\ell\overline{\nu}$ decays. The impact of the selection criteria on the m_X distribution is illustrated on MC in Fig. 2a. We determine $R_{u/sl}$ from N_u, the observed number of $b \to u$ events, and N_{sl}, the number of events with at least one charged lepton:

$$R_{u/sl} = \frac{\mathcal{B}(\overline{B} \to X_u\ell\overline{\nu})}{\mathcal{B}(\overline{B} \to X\ell\overline{\nu})} = \frac{N_u/(\varepsilon^u_{sel}\varepsilon^u_{m_X})}{N_{sl}} \times \frac{\varepsilon^{sl}_l\varepsilon^{sl}_t}{\varepsilon^u_l\varepsilon^u_t}. \quad (4)$$

Here $\varepsilon^u_{sel} = (34.2 \pm 0.6)\%$ is the efficiency for selecting $\overline{B} \to X_u\ell\overline{\nu}$ decays with all analysis requirements, $\varepsilon^u_{m_X} = (73.3 \pm 0.9)\%$ is the fraction of signal events with $m_X < 1.55\,\mathrm{GeV}/c^2$, $\varepsilon^{sl}_l/\varepsilon^u_l = 0.887 \pm 0.008$ corrects for the difference in the efficiency due to the lepton momentum cut for $\overline{B} \to X\ell\overline{\nu}$ and $\overline{B} \to X_u\ell\overline{\nu}$ decays, and $\varepsilon^{sl}_t/\varepsilon^u_t = 1.00 \pm 0.04$ accounts for a possible efficiency difference in the B_{reco} reconstruction in events with $\overline{B} \to X\ell\overline{\nu}$ and $\overline{B} \to X_u\ell\overline{\nu}$ decays.

We derive N_{sl} from a fit to the m_{ES} distribution shown in Fig. 2b. The fit uses an empirical description [13] of the combinatorial background from continuum and $B\overline{B}$ events, together with a narrow signal [14] peaked at the B meson mass. The residual background in N_{sl} from misidentified leptons and semileptonic charm decays amounts to 6.8% and has been subtracted. We obtain N_u from the m_X distribution with a χ^2 fit to the sum of three contributions: signal, background N_c from $\overline{B} \to X_c\ell\overline{\nu}$, and a background of less than 1% from other sources (misidentified leptons, secondary τ and charm decays).

In each bin of the m_X distribution, the combinatorial B_{reco} background is subtracted on the basis of a fit to the m_{ES} distribution. Figure 3a shows the m_X distribution with the results of the fit superimposed. The fit reproduces well the data having a $\chi^2/dof = 7.6/6$. In the fit, the first bin is chosen to contain all events with m_X less than $1.55\,\mathrm{GeV}/c^2$ while the other bins are chosen in order to separate the contribution from each resonant $\overline{B} \to X_c\ell\overline{\nu}$ mode. The m_X cut, set at $1.55\,\mathrm{GeV}/c^2$, has been optimized minimizing the total error. Figure 3b shows the m_X distribution after background subtraction with finer binning. Table 1 summarizes the results of fits with different requirements on m_X, for electrons and muons, for neutral and charged B_{reco} candidates, and for different ranges of the B_{reco} purity, $\mathcal{P}$. The results are all consistent within the uncorrelated statistical errors.

We have performed extensive studies to determine systematic uncertainties. We use events with charged and neutral kaons in the recoil of the B_{reco} candidate as a control sample to assess that the background from $\overline{B} \to X_c\ell\overline{\nu}$ events is properly described. The relative systematic error (Δ_r) due to the selection criteria related to the reconstruction of particles in the event is $\Delta_r = 8.5\%$. The uncertainty of the B_{reco} combinatorial background subtraction is estimated by varying the signal shape function ($\Delta_r = 3.8\%$). The impact of the binning is studied by changing the binning for $m_X > 1.55\,\mathrm{GeV}/c^2$ ($\Delta_r = 2.9\%$). The branching fractions of $B \to D^{(*,**)}\ell\nu$ and of inclusive and exclusive D mesons decays are varied within the world aver-

Table 1. Fit results for several data samples.

Sample	N_{sl}	N_u	N_c	$R_{u/sl}$ (%)
$m_X < 1.55\,\mathrm{GeV}/c^2$	32210 ± 233	167 ± 21	99 ± 6	1.97 ± 0.25
$m_X < 1.40\,\mathrm{GeV}/c^2$	32210 ± 233	134 ± 19	64 ± 4	1.77 ± 0.25
$m_X < 1.70\,\mathrm{GeV}/c^2$	32210 ± 233	191 ± 26	170 ± 11	2.11 ± 0.29
neutral B_{reco}	11582 ± 133	76 ± 13	21 ± 3	2.46 ± 0.43
charged B_{reco}	20583 ± 191	91 ± 16	77 ± 5	1.68 ± 0.30
Electrons	18261 ± 173	99 ± 15	48 ± 4	2.26 ± 0.35
Muons	13934 ± 157	67 ± 14	47 ± 4	1.66 ± 0.36
$\mathcal{P} > 80\%$	4491 ± 68	19 ± 7	13 ± 2	1.59 ± 0.56
$50\% < \mathcal{P} < 80\%$	13298 ± 141	65 ± 13	46 ± 3	1.85 ± 0.37
$\mathcal{P} < 50\%$	14122 ± 170	82 ± 15	38 ± 3	2.21 ± 0.40

age uncertainties [15] (Δ_r = 4.4%). The limited amount of simulated events causes an uncertainty Δ_r = 5.1%. The uncertainty in the hadronization of the final state of $\overline{B} \to X_u \ell \overline{\nu}$ events is determined by measuring $R_{u/sl}$ in bins of charged and neutral multiplicities and performing the fit using only the nonresonant signal model instead of the hybrid model(Δ_r = 3.0%). We also vary the branching fractions for charmless semileptonic B decays by one standard deviation [15](Δ_r = 2.8%). The fraction of signal events with $s\overline{s}$ contents is varied by 100% for the exclusive component and by 30% for the inclusive one [16](Δ_r = 3.7%). In the determination of ε^u_{sel} and $\varepsilon^u_{m_X}$ we allow the nonperturbative parameters to vary according to $\overline{\Lambda}$ = 0.480 ± 0.120 GeV and $\lambda_1 = -0.300 \pm 0.105\,\mathrm{GeV}^2$, obtained by scaling the results in [17] to $O(1/m_b^2, \alpha_s)$ in order to match the nonresonant MC generator [8]. We take into account the correlation of −0.8 between $\overline{\Lambda}$ and λ_1(Δ_r = 17.5%).

We combine the errors related to the detector and the signal and background modeling errors quadratically into the systematic error and obtain $R_{u/sl} = 0.0197 \pm 0.0027 \pm 0.0023 \pm 0.0034$, where the errors are statistical, systematic, and theoretical related to the efficiency determination and extrapolation to the full m_X range respectively. Combining the ratio $R_{u/sl}$ with the measured inclusive semileptonic branching fraction of $\mathcal{B}(\overline{B} \to X\ell\overline{\nu})$ = (10.87 ± 0.18(*stat*) ± 0.30(*sys*))% [12], we obtain $\mathcal{B}(\overline{B} \to X_u \ell \overline{\nu}) = (2.14 \pm 0.29 \pm 0.26 \pm 0.37) \times 10^{-3}$. Using the relation in [15] and the average B lifetime of τ_B = 1.608 ± 0.016 ps [15] we find

$$|V_{ub}| = (4.52 \pm 0.31 \pm 0.27 \pm 0.40 \pm 0.25) \times 10^{-3} \qquad (5)$$

The first error is statistical, the second refers to the experimental systematic uncertainty, the third gives the theoretical uncertainty on the extrapolation of $R_{u/sl}$ to the full m_X range, and the last error combines quadratically the perturbative and nonperturbative uncertainties in the extraction of $|V_{ub}|$ from the total decay rate.

3 Conclusions

Two different approaches for the extraction of $|V_{ub}|$ CKM matrix element have been presented. The analysis based on m_X gives currently the most precise determination of $|V_{ub}|$.

This is primarily due to specific advantages of this technique: large phase-space acceptance and high purity of the sample (signal over background ratio ∼ 1.7). The two results are consistent and they are in agreement with previous inclusive measurements [18].

References

1. N. Cabibbo, Phys. Rev. Lett. **10**, 531 (1963); M. Kobayashi and T. Maskawa, Prog. Th. Phys. **49**, 652 (1973).
2. M. Battaglia *et al.*, "The CKM matrix and the unitarity triangle," arXiv:hep-ph/0304132, 100 (2002)
3. The *BABAR* Collaboration, B. Aubert *et al.*, Nucl. Instrum. Methods. **A479**, 1 (2002).
4. S. Agostinelli *et al.* [GEANT4 Collaboration], SLAC-PUB-9350, CERN-IT-2002-003 (2002)
5. I.I. Bigi, M. Shifman, and N.G. Uraltsev, Annu. Rev. Nucl. Part. Sci. **47**, 591 (1997); J. E. Duboscq *et al.* [CLEO Collaboration], Phys. Rev. Lett. **76**, 3898 (1996).
6. D. Scora and N. Isgur, Phys. Rev. D **52**, 2783 (1995).
7. J.L. Goity and W. Roberts, Phys. Rev. **D51**, 3459 (1995).
8. F. De Fazio and M. Neubert, JHEP **9906**, 017 (1999).
9. T. Sjöstrand, Comput. Phys. Commun. **82**, 74 (1994).
10. G.C. Fox and S. Wolfram, Phys. Rev. Lett. **41**, 1581 (1978).
11. The CLEO Collaboration, A. Bornheim *et al.*, hep-ex/0202019 (2002).
12. B. Aubert *et al.* [BABAR Collaboration], Phys. Rev. D **67**, 031101 (2003).
13. H. Albrecht *et al.* [ARGUS Collaboration], Z. Phys. C **48**, 543 (1990).
14. T. Skwarnicki [Crystal Ball Collaboration], DESY F31-86-02.
15. K. Hagiwara *et al.* [Particle Data Group Collaboration], Phys. Rev. D **66**, 010001 (2002).
16. M. Althoff *et al.* [TASSO Collaboration], Z. Phys. C **27**, 27 (1985). W. Bartel *et al.* [JADE Collaboration], Z. Phys. C **20**, 187 (1983). V. Luth *et al.*, Phys. Lett. B **70**, 120 (1977).
17. D. Cronin-Hennessy *et al.* [CLEO Collaboration], Phys. Rev. Lett. 87:251808, 2001.
18. R. Barate *et al.* [ALEPH Collaboration], Eur. Phys. J. C **6**, 555 (1999); M. Acciarri *et al.* [L3 Collaboration], Phys. Lett. B **436**, 174 (1998); P. Abreu *et al.* [DELPHI Collaboration], Phys. Lett. B **478**, 14 (2000); B. H. Behrens *et al.* [CLEO Collaboration], Phys. Rev. D **61**, 052001 (2000); G. Abbiendi *et al.* [OPAL Collaboration], Eur. Phys. J. C **21**, 399 (2001); A. Bornheim *et al.* [CLEO Collaboration], Phys. Rev. Lett. **88**, 231803 (2002).